



HAL
open science

Bioinspired complexes confined in well-defined capsules: getting closer to metalloenzyme functionalities

Donglin Diao, A. Jalila Simaan, Alexandre Martinez, Cédric Colombar

► To cite this version:

Donglin Diao, A. Jalila Simaan, Alexandre Martinez, Cédric Colombar. Bioinspired complexes confined in well-defined capsules: getting closer to metalloenzyme functionalities. *Chemical Communications*, In press, 10.1039/d2cc06990c . hal-04047768

HAL Id: hal-04047768

<https://hal.science/hal-04047768>

Submitted on 27 Mar 2023

HAL is a multi-disciplinary open access archive for the deposit and dissemination of scientific research documents, whether they are published or not. The documents may come from teaching and research institutions in France or abroad, or from public or private research centers.

L'archive ouverte pluridisciplinaire **HAL**, est destinée au dépôt et à la diffusion de documents scientifiques de niveau recherche, publiés ou non, émanant des établissements d'enseignement et de recherche français ou étrangers, des laboratoires publics ou privés.

ChemComm

Chemical Communications

Accepted Manuscript

This article can be cited before page numbers have been issued, to do this please use: D. Diao, A. J. Simaan, A. Martinez and C. Colombari, *Chem. Commun.*, 2023, DOI: 10.1039/D2CC06990C.



This is an Accepted Manuscript, which has been through the Royal Society of Chemistry peer review process and has been accepted for publication.

Accepted Manuscripts are published online shortly after acceptance, before technical editing, formatting and proof reading. Using this free service, authors can make their results available to the community, in citable form, before we publish the edited article. We will replace this Accepted Manuscript with the edited and formatted Advance Article as soon as it is available.

You can find more information about Accepted Manuscripts in the [Information for Authors](#).

Please note that technical editing may introduce minor changes to the text and/or graphics, which may alter content. The journal's standard [Terms & Conditions](#) and the [Ethical guidelines](#) still apply. In no event shall the Royal Society of Chemistry be held responsible for any errors or omissions in this Accepted Manuscript or any consequences arising from the use of any information it contains.

ARTICLE

Bioinspired complexes confined in well-defined capsules: getting closer to metalloenzyme functionalities.Donglin Diao,^a A. Jalila Simaan,^a Alexandre Martinez^a and Cédric Colombar^{*a}Received 00th January 20xx,
Accepted 00th January 20xx

DOI: 10.1039/x0xx00000x

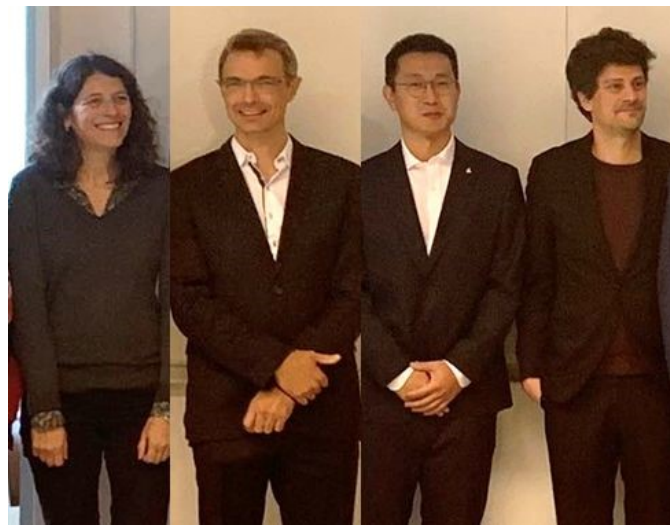
Reproducing the key features offers by metalloprotein binding cavities is an attractive approach to overcome the main bottlenecks of current open artificial models (in terms of stability, efficiency and selectivity). In this context, this Feature Article brings together selected examples of recent developments in the field of confined bioinspired complexes, with an emphasis on the emerging hemicryptophane caged ligands. In particular, we focused on (1) the strategies allowing insulation and protection of complexes sharing similarities with metalloproteins active sites, (2) confinement-induced improvement of catalytic efficiencies and selectivities and (3) very recent efforts that have been made toward the development of bioinspired complexes equipped with weakly-binding artificial cavities.

Introduction

Metalloprotein catalysis is particularly inspiring for synthetic chemists because these enzymatic machineries accomplish a broad range of difficult chemical transformations, under mild conditions. Such biological catalysts combine an active site - usually based on bioavailable metal ions (Cu, Fe, Zn, Mn) supported by natural ligands (O, S and N-donors) - with the three-dimensional enzymatic architecture. The latter provides additional interactions at the secondary (and further) coordination sphere level(s). Within metalloenzymes, remarkable structural tuning of the catalytic efficiency is observed thanks to these cavities (or channels) that guide and orient small substrates to the metal active site, promoting

precise selectivity and product release. For instance, it has been experimentally¹ and computationally² evidenced that substrate positioning in *SyrB2*, *WelO5* and *BesD* halogenases, is critical to achieve highly chemo- and regioselective C-H bond functionalization. This specific adjustment between substrate and active-site results from the substrate orientation, thanks to its stabilization by the protein environment (being sensitive to substrate's charge and polarity). These findings suggest that, within the same family of metalloenzymes, active sites and secondary structures might be substrate, enzyme and even reaction specific. The enzymatic pocket is therefore associated with several key structural features that strongly impact metalloprotein catalysis. It allows for protection of the active site and control of its nuclearity, stabilization of highly reactive intermediates, substrate positioning and product release.

^a Aix Marseille Univ, CNRS, Centrale Marseille, iSm2, Marseille, France.
E-mail: cedric.colombar@univ-amu.fr



Donglin Diao (middle-right) completed his PhD on bioinspired complexes confined in hemicryptophane cages, in 2022, under the guidance of C. Colombar, A. Martinez and A. J. Simaan.

Ariane Jalila Simaan (left) obtained her Ph.D. on bioinorganic chemistry with J.-J. Girerd and F. Banse, before joining the group of P. Hildebrandt as postdoc. She is now CNRS research director at Aix-Marseille University with interests in bioinspired catalysis and enzymatic studies.

Alexandre Martinez (middle-left) obtained his Ph.D. on asymmetric catalysis with B. Meunier. He then works on supramolecular chemistry with J. Lacour (as Postdoc) and J.-P. Dutasta (as lecturer). He is now full professor at the Ecole Centrale Marseille with interests in stereochemistry, catalysis, and supramolecular chemistry.

Cédric Colombar (right) completed his Ph.D. on bioinspired catalysis with A. Sorokin. He undertook postdocs on self-assembled cages with M. Costas and X. Ribas and covalent hosts with A. Martinez. Since 2020, he is CNRS researcher at University Aix-Marseille, with interests in Bioinspired Confined Catalysis.



These identified features account for the high specificity, selectivity and efficiency observed with these remarkable catalysts.

Over the past decades, there has been a growing interest for bioinspired chemistry and, in particular, bioinspired catalysis. Since the pioneering work of Breslow^{3,4} and Kimura,⁵ metalloprotein mimics based on artificial complexes have attracted considerable attention. These minimalistic metal-based structures aim at reproducing the essential features of an enzyme active site, without recreating the whole protein scaffold. This approach has been widely reported as an efficient strategy to *i)* reproduce metalloproteins spectroscopic signatures to help understanding the structures and electronical properties of their active sites (structural models); and *ii)* mirror enzymes reactivities to both elucidate reaction mechanisms and nature of metastable intermediates (functional models). The classical bioinspired strategy has firstly focused on the development of complexes reproducing the first-coordination sphere of one (or more) metal ion(s). These open complexes usually lack stability and cannot fully reproduce the high catalytic efficiency and selectivity of enzymes. In order to demonstrate the core role of the enzymatic hydrophobic binding pocket, artificial complexes displaying second coordination sphere^{6, 7, 8} and/or confined within artificial cavities,⁹ have then been targeted. To better reproduce metalloprotein catalysis, these supramolecular artificial catalysts must provide insulation of both substrate and active site from the bulk medium (recognition) and guarantee their preferential arrangement (orientation). The challenge is therefore to reproduce such key features, while keeping a minimalistic structure allowing for simple preparation, high solubility, ease spectroscopic characterization and recyclability.

Artificial catalysts performing reactions identical to those promoted by enzymes, have been extensively reported over the past few years. In several cases, nanomaterials that are unrelated to the principles of biochemistry or enzymatic catalysis, have been described as nanozymes. But it has been recently stressed by the catalytic community, that such inappropriate analogies have led to the overuse of the “bioinspired”, “enzyme mimic” or “nanozyme” terms.^{10,11} To deserve this label, bioinspired models should share some structural characteristics and/or similar mechanisms (active species, substrates, products, kinetics) with the related enzymes.

In this context, this feature article details recent advances on metal complexes resembling a metalloprotein active site and being confined in a well-defined molecular cage structure. It is designed to reflect the “state-of-the-art” of the strategies that have been lately employed to *i)* confine metalloproteins structural models, *ii)* protect reactive active sites and *iii)* reach superior catalytic behaviours by confinement effect. In particular, we summarize our efforts to use hemicryptophane-based complexes as catalytically active confined models with improved efficiency and selectivity. We finally outline our recent progression toward the development of complexes equipped with chiral and functionalized artificial cavities, aiming at getting one step closer to the metalloprotein key

structural features. Supramolecular catalysts based on non-biological metals, artificial metalloenzymes or nanomaterial frameworks (MOF), are beyond the scope of this work which focus on discrete caged artificial models.

Discussion.

Several strategies could be used to confine artificial complexes into three-dimensional architectures. For instance, complexes could be incorporated in a biological streptavidin scaffold¹² or in micelles,¹³ confined within a self-assembled supramolecular cage by mean of host-guest chemistry, or covalently grafted to an organic cage-like unit. In this last category, the metal complex could be situated inside (endo-functionalization) or above the cage structure. For example Costas, Lledó and coworkers reported, in 2018, bio-inspired Fe^{II} and Mn^{II} complexes based of the bis(pyridyl)dipyrroliidine (**pdp**) ligand, attached to a resorcinarene cavitand Fe^{II} / Mn^{II}(**1-pdp**)(OTf)₂.¹⁴ This self-folding deep cavitand provides a well-defined hydrophobic cavity in a very close proximity to the metal center (**Fig. 1**). The structure did not allow for a complete endohedral functionalization of the complex, that is bound to the cavitand by a single acetal bridge. Contrary to its parent complex Fe^{II}(**pdp**)(OTf)₂, the supramolecular complex displays an iron center in a low spin-state, indicating that the presence of the cavitand modulates the metal electronic properties. Interestingly, the resulting supramolecular complex could activate H₂O₂ to perform C-H and C=C bonds oxidations without suffering from product inhibition. However, no improved selectivities were observed compared to the parent “cavitand-free” complex. On this basis, rigid catalyst-host linkages and/or endohedral functionalization of the active site, might be key to allow selectivity enhancement *via* substrate recognition at a near-by hydrophobic cavity.

The two following sections will focus on selected examples of bioinspired complexes confined in the interior of either covalent or self-assembled cages.

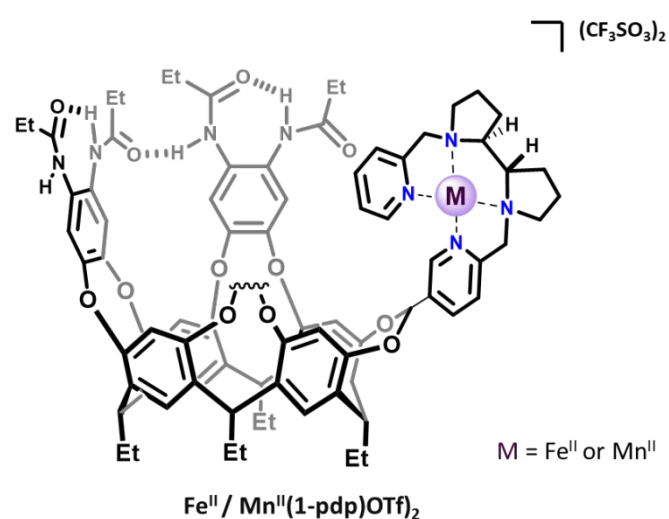


Fig. 1. Representation of cavitand-tailored bioinspired complexes Fe^{II}(**1-pdp**)(OTf)₂ and Mn^{II}(**1-pdp**)(OTf)₂.



Imidazole-based complexes confined in covalent cages.

The imidazole ligand is particularly interesting as it reproduces the histidine-copper coordination found in many mono-oxygenase enzymes (such as particulate methane monooxygenase (pMMO), lytic polysaccharide monooxygenase (LPMO), and tyrosinase). Examples of Zn^{II} complexes based on cyclodextrins,¹⁵ or calix[6]arenes hosts¹⁶ functionalized by imidazole coordinating units, have been reported. However, in the case of these open ligands, the metal was not fully encapsulated in a well-defined cavity. It is not before 2019, that a tripodal azacyclophane cage **2**, decorated by three imidazole ligands pointing toward its interior, was described by the group of Otte (**Fig. 2a**).¹⁷ The design of this organic capsule allows for the coordination of Cu^I, which is situated in the middle of the cage's cavity. A rare T-shaped geometry was revealed by XRD analysis. Interestingly, this T-shaped Cu^I coordination mode, with typical Cu-imidazole distances (1.9 - 2.1 Å), reproduces well the copper-coordination geometry found in some enzymes like LPMOs and pMMO. The authors finally demonstrate that the confined complex Cu^I(**2**)(BF₄) remains catalytically active. It performs the oxidation of benzyl alcohol substrates into aldehydes, in the presence of TEMPO, under air. However, the cage structure does not result in an improvement of the catalytic efficiency, compared to other open copper-based catalysts. Indeed, Cu^I(**2**)(BF₄) and the bipyridine-based Cu(I) catalyst developed by Stahl,¹⁸ display similar efficiency for the oxidation of 4-methoxybenzyl alcohol to 4-anisaldehyde in the presence of N-methylimidazole, with respectively 37% and 39% yields.

The same group reported, in 2021, a derivative of **2** in which one of the imidazole arms is replaced by a carboxylate ligand, resulting in cage **3** (**Fig. 2b**).¹⁹ It should be noted that, compared to previously reported cage-ligands which display a high degree of symmetry, **3** provides an heteroleptic ligand environment. Discovering new strategies to decrease the level of symmetry of caged ligands is particularly important in the context of bioinspired chemistry.²⁰ It indeed allows for introducing non-equivalent ligands around the metal core, as it is observed in several metalloproteins. For example, the well-known α -ketoglutarate (α -KG)-dependent iron oxygenases, display a characteristic 2-histidine-1-carboxylate facial triad at their first coordination sphere. In this context, it is worth noting that the covalent cage-based strategy seems particularly appropriated for the construction of heteroleptic assembly. Indeed, in the case of the self-assembly technique, favoring the formation of a mixed-ligand cage (social sorting) over its homoleptic analogue (one kind of ligand, narcissistic self-sorting) is a more challenging task due to the formation of statistical mixtures of both cage complexes, without selectivity.²¹ The corresponding quasi heteroleptic zinc and iron complexes Zn^{II}(**3**)(SbF₆)₂ and Fe^{II}(**3**)(SbF₆)₂ display an endohedral functionalization provided by the cage structure. This functionalization was unambiguously confirmed by NMR and XRD studies. Importantly, the solid-state structure of Fe^{II}(**3**)(NEt₃)(SbF₆)₂ displays an iron coordination comprising an external molecule of triethylamine (Et₃N, crystallisation co-solvent, **Fig 2b**), the two imidazole moieties,

and the carboxylate unit that bind in an asymmetric, bidentate fashion. This carboxylate coordination, although being unusual for mononuclear artificial complexes, has been interestingly observed in some enzyme active sites (eg naphthalene dioxygenase NDO).²²

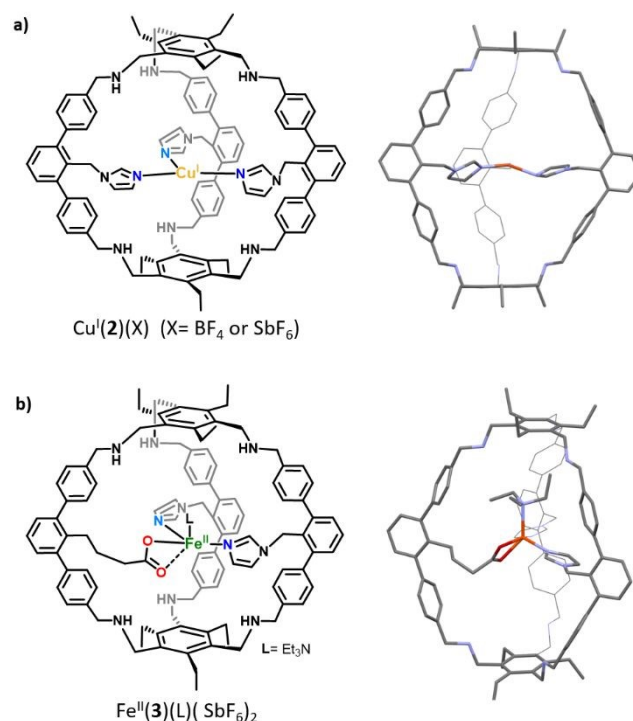


Fig. 2. Schematic representations and XRD structures of (a) the confined copper complex Cu^I(**2**) and (b) heteroleptic caged iron complex Fe^{II}(**3**).

In sharp contrast with most of the “open” carboxylate-based iron complexes, that lead to dimers or polymeric structures,²³ the caged ligand **3** ensures the sole formation of the targeted monomeric Fe complex. These results highlight the benefits of confining complexes within a cage scaffold that offers protection against dimerization or polymerization reactions. This control of the active site nuclearity, *via* insulation of the metal core, is also a characteristic feature of metalloproteins. Finally, although Fe^{II}(**3**)(SbF₆)₂ did not react with dioxygen, it can bind the α -KG cofactor at low temperature (-80°C), resulting in an intermediate that reacts upon warming, in the presence of O₂. These encouraging early findings are particularly interesting for further uses of Fe^{II}(**3**) as functional mimic of non-heme iron oxygenases. This represents a remarkable achievement since Fe(**3**) reproduces, for the first time, the 2-histidine-1-carboxylate facial triad found in many enzymatic active sites, inside a well-defined cavity.

Very lately, this cage-ligand was also used for Cu coordination at the two-imidazoles one-carboxylate ligand, without formation of polymeric species.²⁴ Both caged Cu(I) and Cu(II) complexes have been confined. Interestingly, the cage flexibility allows for the formation of Cu-complexes with different coordinating properties. The Cu(**3**) complex displays a



trigonal planar geometry while its oxidized analogue reveals a Cu^{II} complex in a highly distorted octahedral geometry. The Cu^{II}-coordination comprises the two imidazoles, two external THF molecules and a bidentate carboxylate unit. Upon O₂ exposure of Cu^I(**3**), oxidation of the cage benzamine backbone into benzimine, was observed. Additionally, EPR spectrum of the Cu^{II}(**3**)(PF₆) complex, in the presence of water, displays resemblance with the one of a subunit of a purified particulate methane monooxygenase enzyme (pMMO).²⁵ According to *i*) its two imidazoles one carboxylate triad coordinating Cu(I/II) with two different modes, *ii*) its oxidizing abilities under aerobic conditions and *iii*) its spectroscopic resemblance to the enzyme active site, Cu^{I/II}(**3**) complex could therefore be considered as a promising artificial model of the pMMO active site. Introducing the 2-imidazole-1-carboxylate coordination triad inside an organic cage therefore appears as a particularly encouraging approach, that might lead to new kind of bioinspired catalysts for highly challenging oxidation of strong C-H bonds via O₂ activation.

Bioinspired complexes confined within self-assembled cages.

The second main strategy to confine metal-complexes in an artificial cage architecture, is based on supramolecular hosts obtained *via* the self-assembly technique. Compared to the covalent cages, this approach usually requires less synthetic steps and results in more straightforward preparations and purifications. Although remarkable examples of metal-based catalysts confined in self-assembled cages - for improvement of both their catalytic efficiency and selectivity - have been reported over the past decade,^{26,27,28} very few bioinspired complexes have been included in self-assembled capsules.

A first example of the encapsulation of non-heme Zn^{II}-, Cu^{II}- and Fe^{III}- complexes displaying a bis(2-pyridylmethyl)amine (BPA) coordinating unit, was reported in 2018 by Costas, Ribas and coworkers.²⁹ The supramolecular host was a palladium-based self-assembled nanocage. It consists in two cofacial Zn-porphyrin units linked by four bridging bis-palladium macrocyclic walls, via Pd-carboxylate bonds. A BPA ligand, tailored with a bipyridine unit acting as an anchor binding both Zn-porphyrin units of the cage, was designed. It was demonstrated that the bipyridine anchor successfully drives the encapsulation of the complexes, by host-guest interactions. The BPA unit remains available upon encapsulation, to further coordinate Zn, Cu or Fe biometals in the confined space (Fig. 3a).

Recently, a promising approach consisting in the encapsulation of bioinspired complexes within a purely organic self-assembled capsule, was reported by Colasson and coworkers.³⁰ This organic supramolecular host is a hexameric resorcinarene cage, previously described as powerful nanovessel for supramolecular organocatalysis.^{31,32} It is composed of six resocin[4]arene units and eight water molecules, linked together by a network of sixty hydrogen bonds (Fig. 3b). One key advantage of this capsule is its straightforward preparation that does not require synthetically complex procedures.

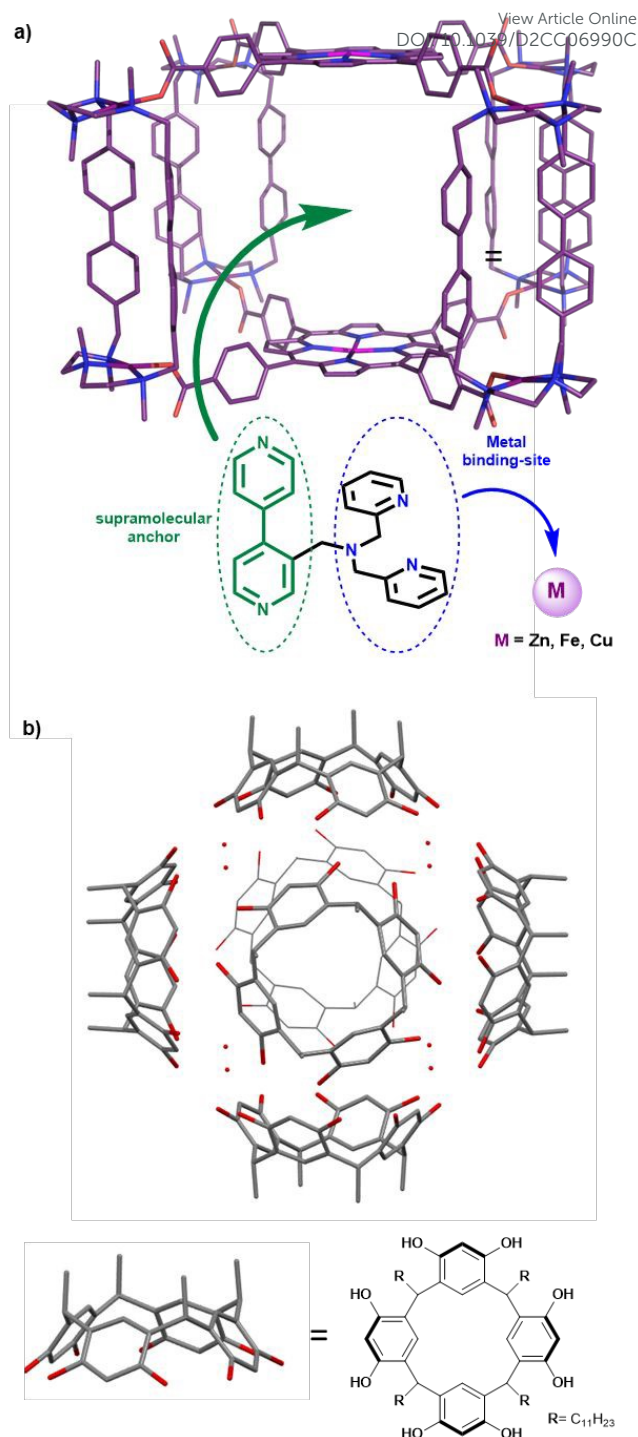


Fig. 3. a) Encapsulation of bioinspired Zn, Fe or Cu complexes within the cavity of a porphyrin-based supramolecular cage, via host-guest interaction. b) Representation of the hexameric self-assembled resorcinarene capsule used for encapsulation of Zn(II) and Cu(II) TPA-based complexes.

Interestingly, in contrast to self-assembled metallacages, this cage is devoid of bridging metal nodes. As a result, it displays a sole metal center that corresponds to the caged bioinspired complexes, resulting in easier characterizations. The authors



demonstrated that Zn(II) and Cu(II) complexes based on the well-known tris(2-pyridylmethyl)amine (TPA) bioinspired ligand, could be efficiently entrapped inside the resorcinarene-based cavity. Encapsulated complexes have been fully characterized by $^1\text{H-NMR}$ analysis coupled with docking simulations. Importantly, the hydrogen-bond donor groups present in the supramolecular assembly (eight water molecules), were found to interact with the azido ligand of an encapsulated $\text{Cu}^{\text{II}}(\text{TPA})(\text{N}_3)$ complex. Studying confined azidocopper(II) adducts is particularly interesting because they are known as structural and electronic analogues of the end-on superoxo intermediate ($\text{Cu}^{\text{II}}\text{O}_2^-$) found in several copper-monoxygenases. Its stabilization, by the second coordination sphere offered by the cage, is therefore particularly encouraging toward further applications of such Cu(I) confined bioinspired complexes, as O_2 activating model catalysts.

Confined Cu(I) complexes as enhanced O_2 activating catalysts.

In biology, vital oxidation and oxygenation reactions are performed by O_2 activating metalloenzymes. Copper- or iron-containing oxidase and oxygenase are indeed able to perform challenging reaction (eg CH_4 oxidation), by generating highly reactive metastable intermediates arising from the activation of O_2 . In this context, the enzyme cavity is essential to stabilize these active species and avoid undesired side reactions such as thermodynamically favored formation of O-bridged dimers. A typical example of this key nuclearity control is the stabilization of $\text{Cu}^{\text{II}}(\text{O}_2^-)$ intermediates by the enzyme cavity of Cu-based oxygenases and oxidases.³³ Indeed, in the absence of steric protection, the instable mononuclear cupric superoxide specie is easily converted to peroxo-bridged dicopper(II) complexes. As a consequence, O_2 activation at open artificial $\text{Cu}^{\text{I}}(\text{TREN})$ or $\text{Cu}^{\text{I}}(\text{TPA})$ models, usually results in the formation of less reactive $[(\text{Cu}(\text{L}))_2(\text{O}_2)]$ peroxo dimers (Fig 4).^{34, 35, 36}

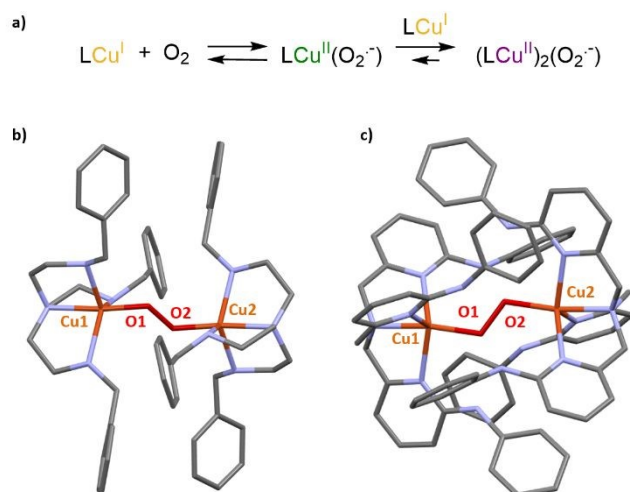


Fig. 4. a) Formation of primary and secondary O_2 adducts arising from O_2 activation at open Cu(I) complexes. XRD structures of $[(\text{Cu}(\text{L}))_2(\text{O}_2)]$ peroxo dimers observed upon O_2 activation at b) $\text{Cu}^{\text{I}}(\text{TREN})$ and c) $\text{Cu}^{\text{I}}(\text{TPA})$ derivatives.

This undesired dimerization could be avoided by using i) very low temperatures,^{37,38} ii) open Cu(I) ligands with significant steric shield,³⁹ and iii) caged bioinspired Cu(I) complexes.

It is in this last category that Reinaud et al. have reported calix[6]arene-caged Cu(I) complexes for O_2 activation studies.⁴⁰ $\text{Cu}^{\text{I}}(\text{TREN})$ and $\text{Cu}^{\text{I}}(\text{TPA})$ units have been connected to the calix[6]arene cap, via methylene bridges, to respectively form the caged complexes $\text{Cu}^{\text{I}}(\mathbf{4})$ ⁴¹ and $\text{Cu}^{\text{I}}(\mathbf{5})$ ⁴² (Fig. 5).

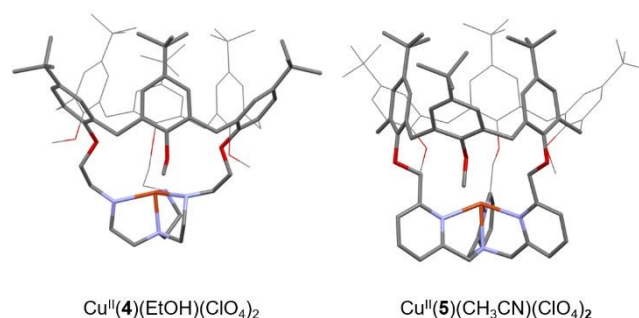


Fig. 5. Views of the XRD structures of Cu^{II} complexes based on the **4** and **5** calix-arene-based ligands. Counter-ions and bounded molecules of solvent (EtOH and CH_3CN respectively), have been omitted for clarity.

Insulation of the Cu core inside the cage-ligands **3** and **4** interestingly prevents the formation of thermodynamically favored peroxo dimers. Instead, it was demonstrated that $\text{Cu}^{\text{I}}(\mathbf{4})$ and $\text{Cu}^{\text{I}}(\mathbf{5})$ could activate O_2 to perform intramolecular oxidation of a methylene $-\text{CH}_2-$ linker. This four-electron oxidation is mediated by the cupric superoxide intermediate $\text{Cu}^{\text{II}}(\mathbf{4/5})(\text{O}_2^-)$, arising from O_2 activation. It results in stable Cu^{I} complexes with a mono-oxidized ligand $\mathbf{4}=\text{O}$ or $\mathbf{5}=\text{O}$ displaying an ester moiety (Fig. 6). It should be noted that the TPA-based complex $\text{Cu}^{\text{I}}(\mathbf{5})$ was less reactive than its TREN analogue. Indeed, $\text{Cu}^{\text{I}}(\mathbf{5})$ solely activates O_2 when used in the solid state. This behavior could be explained by the presence of encapsulated solvent molecule within the cavity of **5**, preventing reaction of the Cu^{I} center with O_2 , in solution.

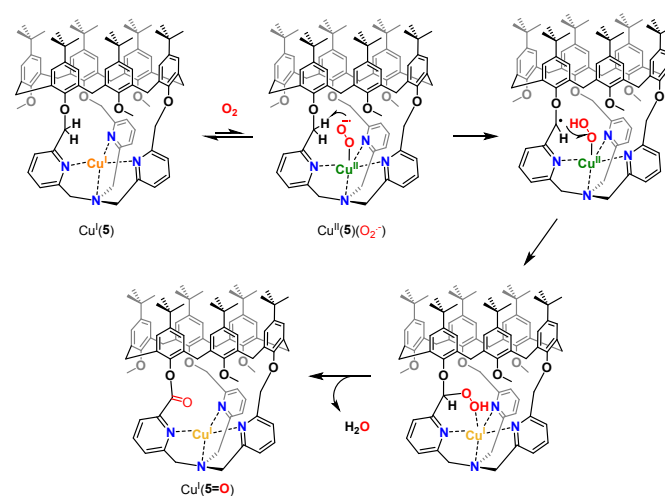


Fig. 6. Proposed mechanism for intramolecular C-H bond oxidation upon O_2 activation at $\text{Cu}^{\text{I}}(\mathbf{5})$. Similar pathway is proposed for $\text{Cu}^{\text{I}}(\mathbf{4})$.



These results clearly indicate that isolating highly reactive intermediates, within well-defined capsules, could be an efficient strategy to reach other reactivity than the one observed in bulk solution. In these cases, confining the biorelevant $\text{Cu}^{\text{II}}(\text{O}_2^-)$ intermediate, prevents the formation of peroxy dimers, to the profit of an O_2 -mediated C-H oxidation reaction. However, this reactivity was limited to intramolecular oxidations. The development of caged O_2 activating catalysts, able to perform C-H oxidation on external substrates, with several turnover numbers, is therefore still needed.

It should be noted that controlling the active site nuclearity via cage-like ligands, have also been used to reach the activation of another important gas: dinitrogen (N_2). Small tripodal cages of the cyclophane-type, displaying two or three identical ligands, have been used to respectively template the formation of bi-⁴³ and trinuclear⁴⁴ iron clusters. The caged-ligands do not only account for the formation of multinuclear complexes, but also impose specific steric constraints and N_2 -coordination modes that allow for unprecedented examples of cleavage of the N_2 triple bond at multimetallic complexes.

Catalytically-active caged models with improved efficiencies.

Hydrogenases-inspired catalysts represent an interesting class of artificial models that have been confined into artificial cages, to improve their efficiency. The first attempt of confining small models of the $[\text{FeFe}]$ -hydrogenases active site, was reported in 2010. Two β -CD cyclodextrins, assembled via a sodium bridge, were used as the host in $(\text{Fe}_2\text{S}_2)(\beta\text{-CD})_2\text{Na}$. In this system, the typical Fe_2S_2 cluster was functionalized at its S-to-S linker, by an aryl sulfonate unit. This anchoring group was used to further include the cluster in the bis-cyclodextrin hydrophobic channel (Fig 7a.). However, the confined model resulted in a less efficient proton reduction, that was attributed to the architecture rigidity that hampers essential rearrangement of the $[\text{Fe-Fe}]$ core.⁴⁵

More recently, Reek and co-workers have extended their initial work - on the encapsulation of single hydrogenases mimics in a metallacage aiming at accessing lower overoxidation potentials⁴⁶ - toward larger metal-based nanospheres that could incorporate multiple hydrogenases active sites.⁴⁷ The $\text{M}_{12}\text{L}_{24}$ Fujita-type nanosphere $\text{Pd}_{12}(\mathbf{6})_5(\mathbf{7})_{19}$ was used to confine five $[\text{Fe}_2\text{S}_2]$ clusters in an ammonium-rich nano-environment. This large metallacage is based on two different bis(pyridyl) ditopic ligands bridged with Pd metal nodes, offering a very wide cavity (5 nm diameter). It arises from the combination of ligands **6** and **7**, being respectively appended with a $[\text{Fe}_2\text{S}_2]$ cluster and an ammonium unit (Fig. 7b). Inside the nanosphere cavity, the five diiron catalysts are therefore surrounded by a proton-rich environment provided by the nineteen **7**. Interestingly, this particular supramolecular environment results in enhanced electrocatalytic proton reduction performances. This positive confinement effect was attributed to the conjunction of two factors: *i*) insulation of the catalyst that reduces the catalytic overpotential and *ii*) preorganization of the proton substrate and intermediates stabilization, arising from the co-confinement of the

ammonium salts. This remarkable enhancement of catalytic efficiency underlines the benefits of combining cage-like hosts with a functionalized second coordination sphere. On this basis, decorated cavities reproducing the key amino-acid residues found around the enzyme active site, appear as a key feature for future progression in the field of bioinspired catalysis.

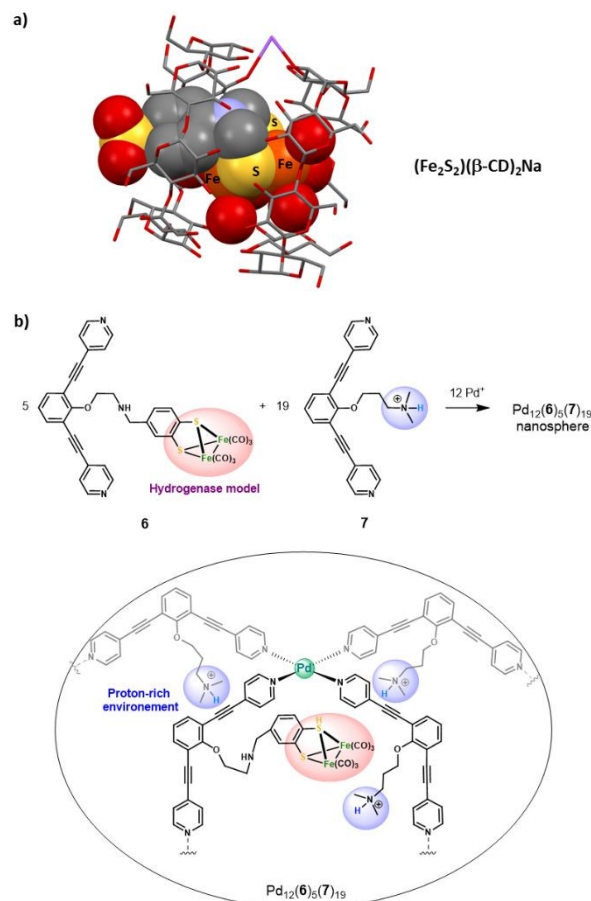


Fig. 7. a) Representation of the XRD structure of $(\text{Fe}_2\text{S}_2)(\beta\text{-CD})_2\text{Na}$. b) Confinement of five hydrogenase mimicking clusters in a proton rich $\text{Pd}_{12}(\mathbf{6})_5(\mathbf{7})_{19}$ nanosphere (top), along with schematic representation of one of five catalytic centers found in the nanosphere (bottom).

Among the different kinds of covalent cage-ligands, the hemicycrophane-type, that is developed in our team, has recently emerged as a useful scaffold for catalytically active bioinspired complexes. Hemicycrophanes are organic covalent cages built from a northern cyclotrimer (CTV) unit, and connected to another C_3 symmetrical moiety, by three linkers. Interestingly, we found that these hosts display a remarkable rigidity-flexibility balance allowing their use as supramolecular catalysts, that usually do not suffer from inhibition by the product.⁴⁸ Hemicycrophanes possess a hydrophobic cavity that have been used for improvement of the efficiency of caged organocatalysts.^{49,50} In particular, these structures take advantage of *i*) their flexibility allowing product ejection, *ii*) their hydrophobic cavity for substrate recognition and *iii*) their chiral CTV cap for building enantiopure hosts. On this basis, we



reasoned that hemicryptophanes might be an interesting platform to confine bioinspired catalysts, inside a hydrophobic cavity. To achieve this goal, tripodal bioinspired ligands have been incorporated at the southern part of the edifice and corresponding complexes have been studied as confined catalysts.

Martinez and coworkers have investigated the enzyme-like kinetic behavior of oxido-vanadium(V)-based catalyst confined in a hemicryptophane displaying binaphthol linkers ($O=V^V$)(**8**) (Fig. 8).⁵¹ ($O=V^V$)(**8**) has been studied as catalyst for sulfides to sulfoxides oxidation, by activation of the cumene hydroperoxide oxidant (CHP). The strong impact of its hydrophobic cavity was evidenced by the observation of a major improvement of the catalytic efficiency, with up to 10000 turnovers. Indeed, a 33-fold faster reaction rate was observed for the caged catalyst, compared to its open analogue devoid of CTV cap ($O=V^V$)(TKA). This confinement effect was explained by efficient hosting of the thioanisol substrate and realising of the oxidized product from the cavity. Remarkably, kinetic studies revealed that the oxidation reaction catalysed by ($O=V^V$)(**8**) obeys the Michaelis-Menten kinetic model enzymatic reactions. Furthermore, inhibition of the reaction was observed in the presence of the tetramethylammonium Me_4N^+ competitive guest which displays strong affinity for the cage cavity thanks to cation- π interactions with the CTV cap (Fig. 8). It should be noted that Michaelis-Menten kinetic behaviour and reaction competitive-inhibition, are two typical features of enzymes, that are very rarely observed with artificial catalysts. Clearly, equipping metal-based oxidation catalysts with the appropriate hydrophobic cavity, is a strong asset to get one step closer to the catalytic behaviour of metalloproteins.

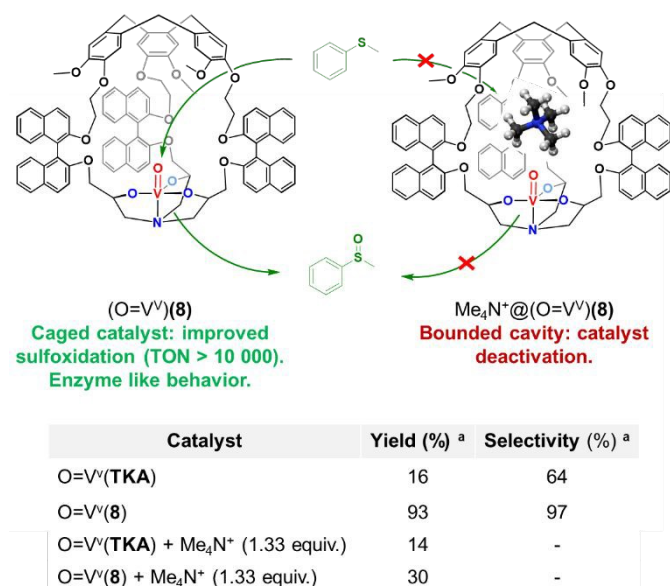


Fig. 8. (Top) Representation of the efficient sulfoxidation observed at caged oxido-vanadium catalyst ($O=V^V$)(**8**) (left), and catalyst inhibition observed upon tetramethylammonium binding at the catalyst cavity (right). (Bottom) Comparison with its open analogue devoid of CTV cap ($O=V^V$)(TKA). ^a Oxidation of thioanisol in the presence of catalyst (1.5 mol%) and CHP (1.0 equiv). for 180 min in CH_2Cl_2 at 0°C.

Improved selectivity by release of primary oxidation products.

DOI: 10.1039/D2CC06990C

Enhancing the selectivity of artificial catalysts, by creating a constrained reaction site, is highly interesting. For example, it was recently demonstrated that equipping iron porphyrin catalyst with a glycoluril-based cage structure,⁵² result in a large selectivity improvement, in CO_2 to CO reduction catalysis.⁵³ This strategy is also particularly attractive to overcome one of the major issues of bioinspired oxidations: controlling the selectivity toward primary oxidation products. Indeed, classical open catalysts usually lack selectivity when applied to the oxidation of very strong C-H bonds. In particular, this is a major difficulty of the direct methane to methanol oxidation. The exceptional stability of CH_4 bonds indeed requires harsh oxidative conditions, that lead to overoxidation of the primary oxidation product (CH_3OH) to undesired formic acid and even CO_2 products.^{54,55} In this context, the bioinspired approach is highly interesting since, in nature, soluble (sMMO) and particulate (pMMO) methane monooxygenases selectively convert CH_4 to CH_3OH , by using confined iron and copper metal ions.

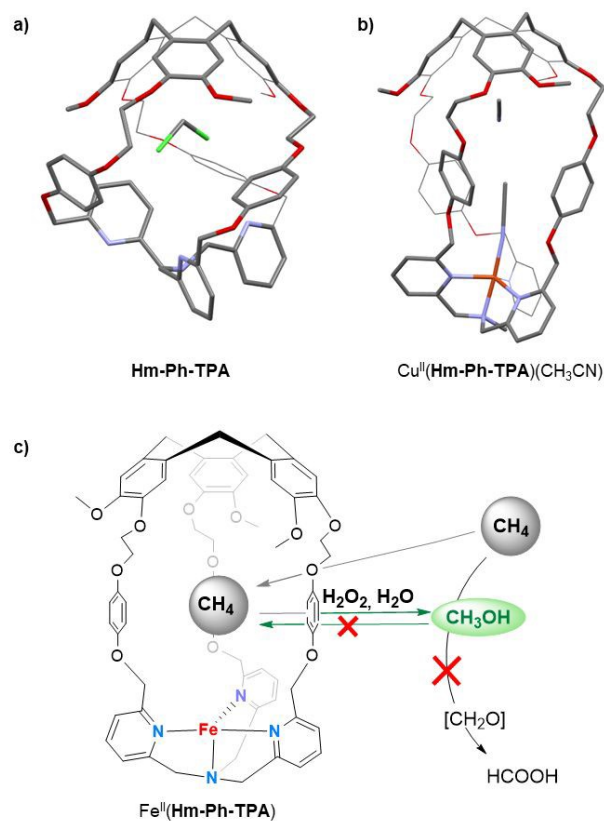


Fig. 9. Representation of the XRD structures of a) Hm-Ph-TPA and b) $Cu^{II}(Hm-Ph-TPA)$. c) Concept of the selective methane to methanol oxidation via H_2O_2 activation at $Fe^{II}(Hm-Ph-TPA)$, in water along with comparison table between the open $Fe(Ph-TPA)$ and the caged catalysts. ^a Selectivity toward primary oxidation products CH_3OH and CH_3OOH .



These enzymes take advantages of their constrained hydrophobic environments that promote methanol release, preventing further overoxidation. By connecting a CTV cap with the tripodal pyridine-based ligand **TPA**, via phenyl linkers, we have prepared the caged bio-inspired Cu and Fe complexes $\text{Cu}^{\text{I}}/\text{Fe}^{\text{II}}(\text{Hm-Ph-TPA})$ (**Fig. 9**). These H_2O_2 -activating catalysts have been further applied in C-H bond oxidation reactions with enhanced selectivity. Inspired by the superior efficiency of copper(II) hemicryptophane catalysts in the oxidation of cyclohexane C-H bonds (via H_2O_2 activation),⁵⁶ we indeed reasoned that such caged catalysts could also favour methanol ejection from the cage cavity, preventing overoxidation. The complexes were supported onto silica and studied as heterogeneous H_2O_2 -activating catalysts for CH_4 to CH_3OH oxidation, in water. We interestingly demonstrated that equipping the iron complex $\text{Fe}(\text{TPA})$, with the hemicryptophane cavity, indeed limits CH_3OH overoxidation.⁵⁷ The $\text{Fe}^{\text{II}}(\text{Hm-Ph-TPA})$ catalyst displayed a 4-fold increase of the yield in mono-oxidized products compared to its "open" analogue. Such confinement effect was explained by preferential binding of the hydrophobic CH_4 and release of the more polar CH_3OH to the bulk water solvent.

Although these results reveal the benefits of the endohedral hydrophobic cavity in terms of selectivity, very low TON (<10) were observed. Therefore, pursuing these studies toward caged catalysts displaying more reactive active site, appear as an encouraging perspective to achieve both efficient and selective CH_4 to CH_3OH conversion.

Reaction in complex media.

A key structural feature of metalloproteins is their ability to catalyse specific reactions within the complex *in-vivo* media. For example, several copper-containing enzymes uses Cu^{I} centers to activate O_2 , without suffering from the competition of external biological Cu^{I} -ligands such as biothiols (like Glutathione or Cysteine). Interactions between these biothiols and the Cu^{I} center are indeed prevented by having the metal core deeply buried inside the metalloprotein scaffold. Artificial Cu^{I} -catalysts for *in-vivo* chemistry have recently attracted considerable attention. Reported examples aimed at achieving *i)* reactive oxygen species (ROS) production at $\text{Cu}^{\text{I}}/\text{Cu}^{\text{II}}$ -cycling complexes for anticancer drugs development,^{58,59} or *ii)* Cu -catalyzed azide-alkyne cycloaddition (CuAAC) bioconjugation reactions.⁶⁰ However, the development of catalysts that remain active in the complex mixtures found in living media (containing strong Cu^{I} biological chelators), remains highly challenging. Indeed, deactivation of open Cu -catalysts *via* copper-coordination by external nucleophiles is the main explanation for their usual scarce *in-vivo* efficiency. For example, Cu^{I} coordination by the glutathione reduced (GSH) tripeptide is considered as the main event preventing CuAAC bioconjugation reactions in living cells.⁶¹

On this basis, we wondered if building an organic hemicryptophane cage around the widely used $\text{Cu}^{\text{I}}(\text{TBTA})$ CuAAC catalysts (**TBTA** = tris(benzyltriazolemethyl)amine), could result in an efficient protection of the Cu^{I} core. We therefore

reported, in 2021, the first covalent caging of the canonical **TBTA** ligand, using the hemicryptophane cage **Hm-TBTA**.⁶² To evaluate the benefits of the cage-shielded structure, the catalytic behaviours of the open $\text{Cu}^{\text{I}}(\text{TBTA})$ and caged $\text{Cu}^{\text{I}}(\text{Hm-TBTA})$ catalysts, in the presence of external bulky Cu -ligands, were compared (**Fig. 10**). Both catalysts were engaged in a typical CuAAC benchmark reaction. We firstly demonstrated that the flexibility of the caged ligand allows for product ejection from its cavity. Indeed, triazole products were not blocked within the cage and catalytic transformations were observed with 99 TON. This behaviour contrasts with other confined CuAAC Cu^{I} -catalysts based on cucurbit[7]uril host, which displays a complete suppression of the catalytic behavior,⁶³ highlighting the benefits of the hemicryptophane structure. Remarkably, the confined catalyst was tolerant to the presence of the notorious glutathione reduce inhibitor.

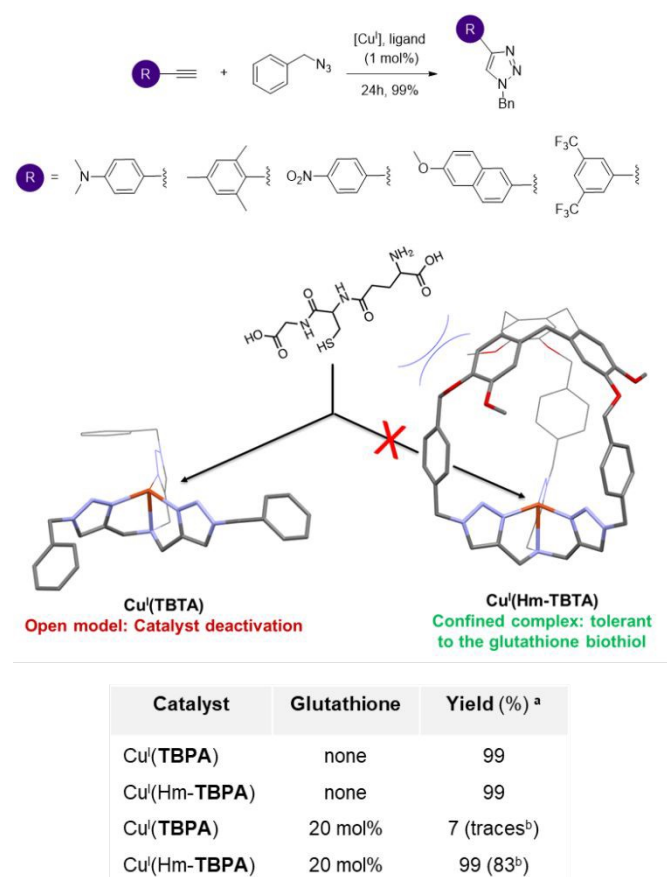


Fig. 10. Typical CuAAC reactions catalysed by $\text{Cu}^{\text{I}}(\text{Hm-TBTA})$ with quantitative yields (**top**). CuAAC reaction in the presence of the glutathione biothiol: no catalyst inhibition was observed in the case of the caged complex, contrary to the classical open CuAAC catalyst (**bottom**). ^a Catalyst (1 mol%), MeOH/ CH_2Cl_2 1:10, 25°C, argon atmosphere. ^b Isolated yields.

Indeed, the catalytic efficiency of $\text{Cu}^{\text{I}}(\text{Hm-TBTA})$ remained unchanged even in the presence of 20 equivalents of GSH. Under identical conditions, the catalytic efficiency of the canonical open complex $\text{Cu}^{\text{I}}(\text{TBTA})$ was totally suppressed. Moreover, it was previously reported that the addition of only 2 equivalents of GSH was sufficient to inhibit the catalytic



activity of common tris(triazole)-based CuAAC catalysts.⁶⁴ This behaviour also highlights the benefits of the hemicryptophane flexibility-rigidity balance, since Cu-catalysts encapsulated in azacryptand caged ligands were found to be too structurally flexible to efficiently prevent GSH-induced deactivation of the confined catalysts.⁶⁵

Clearly, confining Cu^I active center inside a CTV-based organic cage offers an efficient protection of the active core against its deactivation by the abundant biological Cu(I) ligand, GSH. This strategy, inspired by Cu-containing metalloprotein pockets, is therefore encouraging for the future forging of artificial metal catalysts efficiently operating in complex biological media.

Toward chiral and functionalized artificial cavities.

Stereoselective recognitions of natural substrates are particularly important events for several natural biochemical catalytic processes. In order to reproduce these selective bindings, the preparation of chiral artificial cages have recently attracted considerable attention.⁶⁶ In this context, the hemicryptophane structure is particularly interesting due to the inherent chirality of the CTV cap, which display a *M* or *P* configuration.^{67,68} Our team has developed remarkable preparation and/or purification technics (eg chiral HPLC resolution of enantiomers), allowing for the efficient preparation of enantiopure hemicryptophanes cages at the gram scale.⁶⁹ These hosts could be considered as promising ligands for the preparation of both caged and enantiopure bioinspired complexes.⁷⁰

We therefore wondered: could the chirality of the northern CTV cap be transferred to a southern bioinspired ligand? To answer this question, we have designed hemicryptophane **Hm-CH₂-TPA**, displaying a southern tris(2-pyridylmethyl)amine (TPA) ligand and a CTV unit, linked in close proximity by short methylene -CH₂- spacers. We investigated if a helical arrangement of the TPA could be induced and controlled by the CTV cap, in this structurally contracted cage (**Fig. 11.**). Indeed, controlling the interconversion of the TPA's pyridines could lead to a propeller-like arrangement of the ligand, which becomes a chiral coordinating unit. We were pleased to observe that such propagation of the CTV chirality could indeed be achieved in **Hm-CH₂-TPA**. The CTV unit was found to control the ligand helicity, with the *P*-CTV imposing a right-handed propeller arrangement of the TPA's pyridines (while the *M*-CTV provides a left-handed arrangement).

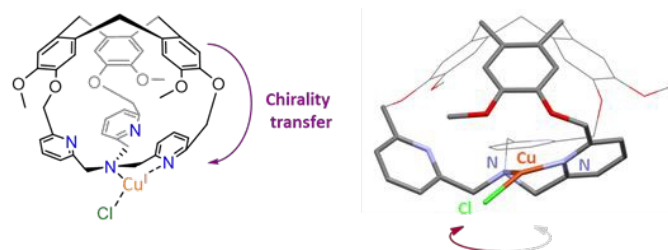


Fig. 11. Schematic representation of the chirality transfer observed in *M*-Cu^I(**Hm-CH₂-TPA**)(Cl) (left), along with view of its XRD structure (right).

Importantly, this chirality transfer remains intact in the corresponding Cu^I complex *M*-Cu^I(**Hm-CH₂-TPA**)(Cl). XRD, ¹H-NMR, ECD analysis and DFT calculations confirm the formation of a highly unusual T-shaped TPA-Cu^I core with a controlled helicity.^{71,72} Connecting tripodal ligands with CTV-based hosts, could be therefore used to reach both optically pure and caged bioinspired complexes, that might find interesting application in enantioselective catalysis.

Another major structural feature of metalloenzymes is their binding cavities that guides the reactivity and selectivity of reactions via *i*) substrate positioning and *ii*) stabilization of extremely reactive intermediates. Several non-covalent second coordination sphere interactions exist in their hydrophobic channels (electrostatic or hydrogen-bonding interactions, salt-bridges and long-ranges charge-effects). Such weak binding events enable high chemo-, regio- and stereoselectivity by finely positioning the substrate. This behaviour has been demonstrated for both heme,⁷³ and non-heme iron oxygenases.⁷⁴ Particularly important H-bonding interactions are also found in O₂ activating copper-containing metalloproteins. In these systems, H-bonding could account for a stabilization of highly reactive intermediates. The strong impact of bonding second coordination spheres have also been demonstrated with tailored open artificial catalysts.⁷⁵ For instance, Karlin and Solomon reported efficient stabilization of end-on superoxo Cu^{II}(TPA)(O₂⁻) intermediates by introducing H-bonding group at the second coordination sphere of the canonical TPA ligand.^{76,77,78} Furthermore, highly precise and predictable C-H oxidation reactions, enable by substrate positioning at crown-ether tailored Mn or Fe bioinspired catalysts, was reported by Costas, Olivo and Di Stefano.^{79, 80, 81} However, despite both progresses in the development of *i*) caged bioinspired complexes and *ii*) open models displaying functional second coordination sphere, the preparation of bioinspired complexes combining a hydrophobic cavity with weak binding units, have been rarely explored.⁸² For instance, impact of functionalized second coordination sphere on metal ion lability and host-guest binding, was very lately evidenced using confined Zn(II) complexes displaying a calix[6]arene-based cavity decorated with phenol or quinone units.⁸³ To better reproduce metalloproteins key structural features, bioinspired catalysts able to precisely orientate substrates inside an artificial cavity, will represent a major breakthrough in the field.

Our first efforts toward construction of such kind of caged complexes, involved the building of a TPA-ligand surmounted with a triazole-decorated cavity. We reasoned that triazole could represent an attractive building block since it is a convenient connecting unit to covalently link the north (CTV) and south (ligand) part of a cage via well-known "click" CuAAC reaction. Additionally, triazoles could be used as H-bond donor moieties. C_{triazole}-H are indeed good H-bond donors that have been, for instance, incorporated in the most efficient chloride-binding covalent cage to date.⁸⁴ We therefore design **Hm-TriA-TPA**, where the bioinspired TPA ligand is connected to the hemicryptophane's CTV by three triazole links (**Fig 12a**). This cage was the first TPA-based ligand surmounted with a C_{triazole}-H H-bonding cavity.⁸⁵ The structure of the corresponding zinc



complex $\text{Zn}^{\text{II}}(\text{Hm-TriA-TPA})$ was elucidated by means of $^1\text{H-NMR}$ and DFT studies. An endohedral functionalization of the $\text{Zn}^{\text{II}}(\text{TPA})$ complex, with the three triazole units remaining available for further H-bonding events, was observed (Fig. 12b). XRD structure of a cage complex was elucidated by replacing zinc with a copper(II) metal ion in $\text{Cu}^{\text{II}}(\text{Hm-TriA-TPA})$. In this case, additional Cu^{II} coordination, by one triazole unit, was observed in the solid state. Interestingly, this Cu-triazole bond could be replaced by coordination of an azide anion at the $\text{Cu}^{\text{II}}(\text{TPA})$ core, liberating the triazole unit (Fig. 12c). As mentioned earlier, TPA-based azidocopper(II) adducts are stable structural analogues of the biological end-on $\text{Cu}^{\text{II}}\text{O}_2^-$ intermediates. They are therefore convenient probes to investigate putative second coordination sphere stabilization via H-bonding. The electronic and vibrational properties of $\text{Cu}^{\text{II}}(\text{Hm-TriA-TPA})(\text{N}_3)$ have thus been compared to that of the analogue $\text{Cu}^{\text{II}}(\text{Me}_3\text{TPA})(\text{N}_3^-)$ adduct devoid of H-bonding units. Remarkably, UV_{vis} and IR analysis reveal respectively a typical blue shift of the azido to Cu^{II} LMCT and an increase of the $\nu(\text{N-N})$ stretching frequency, accounting for a stabilization of the azido adduct by the $\text{C}_{\text{triazole-H}}$ cavity.^{30,76-78}

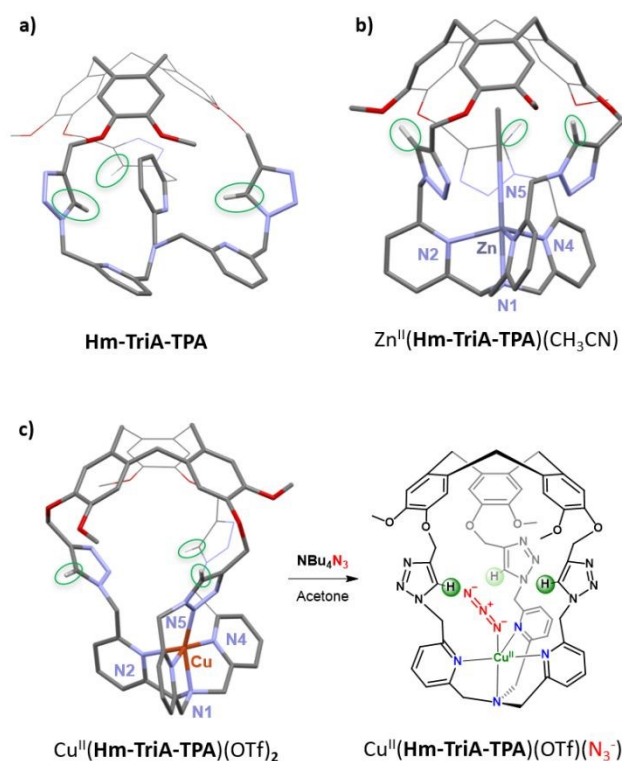


Fig. 12. Views of the DFT structures of **a)** the cage-ligand **Hm-TriA-TPA** and **b)** its corresponding Zn^{II} complex. **c)** View of the XRD structure of $\text{Cu}^{\text{II}}(\text{Hm-TriA-TPA})(\text{OTf})_2$ along with formation of the corresponding azido adduct upon addition of tetrabutylammonium azide.

We were able to show that connecting both parts of a ditopic cage, via triazole linkers, can provide an easy route for confining bioinspired complexes in an H-bonding cavity. In addition to an endohedral functionalisation of the metal core,

we confirmed that the $\text{C}_{\text{triazole-H}}$ bonds, found in the cavity, could engage H-bonding interactions at the second coordination sphere level. This approach therefore opens the way to further artificial catalysts displaying H-bonding cavities, allowing stabilization of reactive metastable intermediates and/or substrate positioning.

Conclusions

With the development of both bioinspired catalysis and supramolecular chemistry, series of well-defined synthetic cage structures have been designed to host enzyme-related artificial complexes. In this Featured Article, we have selected examples of caged complexes reflecting recent efforts in the field of bioinspired catalysis in confined space. We have especially emphasized the confined catalysts based on the emerging hemicryptophane ligands developed in our group. All these systems have been designed to artificially reproduce some key features offered by the enzyme pockets, that have been clearly identified as follow.

(1) Active site protection and reaction in complex media.

The active metal core is usually deeply buried inside the enzyme architecture. This confers protection, in particular against intermolecular reactions between two complexes, resulting in undesired formation of polynuclear species or degradation events. This insulation from the bulk solution also protects the metal core from its deactivation by the external metal chelators found in the complex *in-vivo* media at high concentrations (like biothiols). The ability of organic cage-complexes to avoid the formation of polynuclear O-bridged compounds have been exploited to reproduce *i)* the reactivity and *ii)* the 2-histidine-1-carboxylate facial triad, of important O_2 activating enzymes. Although the key role of the cage structure was clearly evidenced, O_2 activation at caged bioinspired catalysts usually results in an intramolecular oxidation of the ligand. Developing new caged catalysts able to guide this reactivity toward the oxidation of external substrates with strong C-H bonds, could therefore be considered as an important future direction. On another side, hemicryptophane-based complexes have proven useful to obtain catalytically active catalysts operating in the presence of biological strong metal chelators. We therefore believe that this finding opens opportunities to develop artificial catalysts working in living cells for *in-vivo* applications (bioconjugation reactions or drug development).

(2) Hydrophobic cavities for improvement of the catalytic behavior and selectivity.

Besides offering protection, the hydrophobic pocket of enzymes also allows for recognition events leading to highly efficient and selective transformations. Reactions performed by metalloenzymes indeed strongly benefit from the recognition of a specific substrate accompanied with a promoted product-release. Obtaining caged bioinspired catalysts that remain catalytically active, is not an easy task. These systems should be robust enough to avoid cage disassembly, rigid enough to favor substrate recognition, but with a sufficient degree of flexibility allowing product release. Indeed, caged catalysts often suffer from inhibition by the product. As our knowledge on bioinspired



hemicryptophane catalyst increases, we are finding that this cage structure offers a remarkable flexibility-rigidity balance. Bioinspired catalysts surmounted by the hemicryptophane cavity have been successfully applied in oxidation catalysis. The hydrophobic cavity was used to favor accommodation of apolar substrates and promote release of less polar products to avoid overoxidation side reactions. However, in the case of more recalcitrant substrates (like methane), further improvement of the catalytic efficiency, in terms of number of turnovers, are required to get closer to metalloprotein efficiency. In particular our future efforts will be dedicated to combine highly stable capsules with more reactive bioinspired metal cores.

(3) Binding cavities. To precisely control the adjustment between the active site and its co-encapsulated substrate, the sole hydrophobic effect is not sufficient. For instance, catalysis at metalloprotein strongly benefits from their binding pockets that both interact with substrates and active sites. These non-covalent interactions guarantee substrate positioning and stabilization of highly reactive intermediates. Although a relatively large number of bioinspired complexes with discrete cavities have been reported over the past decades, complexes equipped with a functionalized cavity remain rare. The field of confined bioinspired catalysis assisted by weak bonding cavities is in its infancy and remains mainly unexplored. Examples of H-bonding capsules able to stabilize structural (non-reactive) models of bio-relevant metal-based intermediates have been described.^{30, 85} But switching to functional complexes displaying reactivity inside discrete H-bonding confined spaces, is still particularly challenging. In this line, caged catalysts able to control substrate positioning, by mean of substrate-cavity weak bonding, appear as a major perspective to push the limits of current bioinspired confined catalysis.

Conflicts of interest

“There are no conflicts to declare”.

Acknowledgements

This work received support from the French government under the France 2030 investment plan, as part of the Initiative d'Excellence d'Aix-Marseille Université – A*MIDEX (AMX-21-PEP-041).

Notes and references

- 1 R. J. Martinie, J. Livada, W.-C. Chang, M. T. Green, C. Krebs, J. M. Bollinger and A. Silakov, *J. Am. Chem. Soc.*, 2015, **137**, 6912–6919.
- 2 R. Mehmood, V. Vennelakanti and H. J. Kulik, *ACS Catal.*, 2021, **11**, 12394–12408.
- 3 R. Breslow and L. E. Overman, *J. Am. Chem. Soc.* 1970, **92**, 1075–1077.
- 4 R. Breslow, *Acc. Chem. Res.*, 1995, **28**, 146–153.
- 5 T. Koike and E. Kimura, *J. Am. Chem. Soc.* 1991, **113**, 8935–8941.
- 6 D. Vidal, G. Olivo and M. Costas, *Chem. Eur. J.*, 2018, **24**, 5042–5054.
- 7 M. Zhao, H.-B. Wang, L.-N. Ji and Z.-W. Mao, *Chem. Soc. Rev.*, 2013, **42**, 8360–837.
- 8 J. Trouvé, P. Zardi, S. Al-Shehimi, T. Roisnel and R. Gramage-Doria, *Angew. Chem. Int. Ed.* 2021, **60**, 18006–18013.
- 9 C. Bravin, E. Badetti, G. Licini and C. Zonta, *Coord. Chem. Rev.*, 2021, **427**, 213558.
- 10 S. Scott, H. Zhao, A. Dey and T. B. Gunnoe, *ACS Catal.*, 2020, **10**, 14315–14317.
- 11 A. Robert and B. Meunier, *ACS Nano*, 2022, **16**, 6956–6959.
- 12 J. Serrano-Plana, C. Rumo, J. G. Rebelein, R. L. Peterson, M. Barnet and T. R. Ward, *J. Am. Chem. Soc.*, 2020, **142**, 10617–10623.
- 13 K. Chen, M. Zangiabadi and Y. Zhao, *Org. Lett.*, 2022, **24**, 3426–3430.
- 14 D. Vidal, M. Costas and A. Lledo, *ACS Catal.*, 2018, **8**, 3667–3672.
- 15 I. Tabushi and Y. Kuroda, *J. Am. Chem. Soc.*, 1984, **106**, 4580–4584.
- 16 A. Parrot, S. Collin, G. Bruylants and O. Reinaud, *Chem. Sci.*, 2018, **9**, 5479–5487.
- 17 S. C. Bete, C. Würtele and M. Otte, *Chem. Commun.*, 2019, **55**, 4427–4430.
- 18 J. M. Hoover and S. S. Stahl, *J. Am. Chem. Soc.*, 2011, **133**, 16901–16910.
- 19 S. C. Bete and M. Otte, *Angew. Chem. Int. Ed.*, 2021, **60**, 18582–18586.
- 20 C. T. Mc Ternan, J. A. Davies and J. R. Nitschke, *Chem. Rev.*, 2022, **122**, 10393–10437.
- 21 D. Preston, J. E. Barnsley, K. C. Gordon and J. D. Crowley, *J. Am. Chem. Soc.*, 2016, **138**, 10578–10585.
- 22 B. Kauppi, K. Lee, E. Carredano, R. E. Parales, D. T. Gibson, H. Eklund and S. Ramaswamy, *Structure*, 1998, **6**, 571–586.
- 23 S. Friedle, E. Reisner and S. J. Lippard, *Chem. Soc. Rev.*, 2010, **39**, 2768–2779.
- 24 S. C. Bete, L. K. May, P. Woite, M. Roemelt and M. Otte, *Angew. Chem. Int. Ed.*, 2022, DOI:10.1002/anie.202206120.
- 25 R. J. Jodts, M. O. Ross, C. W. Koo, P. E. Doan, A. C. Rosenzweig, B. M. Hoffman, *J. Am. Chem. Soc.* 2021, **143**, 15358–15368.
- 26 M. Raynal, P. Ballester, A. Vidal-Ferran and P. W. N. M. van

View Article Online

DOI: 10.1039/D2CC06990C



- Leeuwen, *Chem. Soc. Rev.*, 2014, **43**, 1734–1787.
- 27 M. Morimoto, S. M. Bierschen, K. T. Xia, R. G. Bergman, K. N. Raymond and F. Dean Toste, *Nat Catal.*, 2020, **3**, 969–984.
- 28 C. García-Simón, R. Gramage-Doria, S. Raoufmoghaddam, T. Parella, M. Costas, X. Ribas and J. N. H. Reek, *J. Am. Chem. Soc.*, 2015, **137**, 2680–2687.
- 29 C. Colomban, V. Martin-Diaconescu, T. Parella, S. Goeb, C. García-Simón, J. Lloret-Fillol, M. Costas and X. Ribas, *Inorg. Chem.*, 2018, **57**, 3529–3539.
- 30 T. Zhang, L. Le Corre, O. Reinaud and B. Colasson, *Chem. Eur. J.*, 2021, **27**, 434–443.
- 31 Q. Zhang, L. Catti and K. Tiefenbacher, *Acc. Chem. Res.*, 2018, **51**, 2107–2114.
- 32 S. Merget, L. Catti, G. M. Piccini and K. Tiefenbacher, *J. Am. Chem. Soc.*, 2020, **142**, 4400–4410.
- 33 C. E. Elwell, N. L. Gagnon, B. D. Neisen, D. Dhar, A. D. Spaeth, G. M. Yee and W. B. Tolman, *Chem. Rev.*, 2017, **117**, 2059–2107.
- 34 K. D. Karlin, S. Kaderli and A. D. Zuberbühler, *Acc. Chem. Res.*, 1997, **30**, 139–147.
- 35 K. Komiyama, H. Furutachi, S. Nagatomo, A. Hashimoto, H. Hayashi, S. Fujinami, M. Suzuki and T. Kitagawa, *Bull. Chem. Soc. Jpn.*, 2004, **77**, 59–72.
- 36 E. W. Dahl, H. T. Dong and N. K. Szymczak, *Chem. Commun.*, 2018, **54**, 892–895.
- 37 R. Trammell, K. Rajabimoghaddam and I. Garcia-Bosch, *Chem. Rev.*, 2019, **119**, 2954–3031.
- 38 J. J. Liu, D. E. Diaz, D. A. Quist and K. D. Karlin, *Isr. J. Chem.*, 2016, **56**, 738–755.
- 39 S. Y. Quek, S. Debnath, S. Laxmi, M. van Gastel, T. Krämer and J. England, *J. Am. Chem. Soc.*, 2021, **143**, 19731–19747.
- 40 N. Le Poul, Y. Le Mest, I. Jabin and O. Reinaud, *Acc. Chem. Res.*, 2015, **48**, 2097–2106.
- 41 G. Izzet, J. Zeitouny, H. Akdas-Killig, Y. Frapart, S. Ménage, B. Douziech, I. Jabin, Y. Le Mest and O. Reinaud, *J. Am. Chem. Soc.*, 2008, **130**, 9514–9523.
- 42 G. Thiabaud, G. Guillemot, I. Schmitz-Afonso, B. Colasson and O. Reinaud, *Angew. Chem. Int. Ed.*, 2009, **48**, 7383–7386.
- 43 J. F. Torres, C. H. Oi, I. P. Moseley, N. El-Sakkout, B. J. Knight, J. Shearer, R. García-Serres, J. M. Zadrozny and L. J. Murray, *Angew. Chem. Int. Ed.* 2022, **61**, e202202329.
- 44 Y. Lee, F. T. Sloane, G. Blondin, K. A. Abboud, R. García-Serres and L. J. Murray, *Angew. Chem. Int. Ed.* 2015, **54**, 1499–1503.
- 45 M. L. Singleton, J. H. Reibenspies and M. Y. Darensbourg, *J. Am. Chem. Soc.*, 2010, **132**, 8870–8871.
- 46 S. S. Nurttilla, R. Zaffaroni, S. Mathew and J. N. H. Reek, *Chem. Commun.*, 2019, **55**, 3081–3084.
- 47 R. Zaffaroni, N. Orth, I. Ivanovic-Burmazovic and J. N. H. Reek, *Angew. Chem. Int. Ed.*, 2020, **59**, 18485–18489.
- 48 D. Zhang, A. Martinez and J.-P. Dutasta, *Chem. Rev.*, 2017, **117**, 4900–4942.
- 49 J. Yang, B. Chatelet, V. Dufaud, D. Héroult, S. Michaud-Chevallier, V. Robert, J.-P. Dutasta and A. Martinez, *Angew. Chem. Int. Ed.*, 2018, **57**, 14212–14215.
- 50 B. Chatelet, L. Joucla, J.-P. Dutasta, A. Martinez, K. C. Szeto and V. Dufaud, *J. Am. Chem. Soc.*, 2013, **135**, 5348–5351.
- 51 D. Zhang, K. Jamieson, L. Guy, G. Gao, J.-P. Dutasta and A. Martinez, *Chem. Sci.*, 2017, **8**, 789–794.
- 52 J. A. A. W. Elemans and R. J. M. Nolte, *Chem. Commun.*, 2019, **55**, 9590–9605.
- 53 A. K. Surendran, G. L. Tripodi, E. Pluhařová, A. Y. Pereverzev, J. P. J. Bruekers, J. A. A. W. Elemans, E. Jan Meijer and J. Roithová, *Nat Sci.*, 2022, e20220019.
- 54 E. V. Kudrik, P. Afanasiev, L. X. Alvarez, G. Blondin, P. Dubourdeaux, M. Clémancey, J.-M. Latour, D. Bouchu, F. Albrieux, S. E. Nefedov and A. B. Sorokin, *Nat. Chem.*, 2012, **4**, 1024–1029.
- 55 A. B. Sorokin, E. V. Kudrik and D. Bouchu, *Chem. Commun.*, 2008, 2562–2564.
- 56 O. Perraud, A. B. Sorokin, J.-P. Dutasta and A. Martinez, *Chem. Commun.*, 2013, **49**, 1288–1290.
- 57 S. A. Ikbāl, C. Colomban, D. Zhang, M. Delecluse, T. Brotin, V. Dufaud, J.-P. Dutasta, A. B. Sorokin and A. Martinez, *Inorg. Chem.* 2019, **58**, 7220–7228.
- 58 A. Santoro, J. S. Calvo, M. D. Peris-Díaz, A. Krężel, G. Meloni, and P. Faller, *Angew. Chem. Int. Ed.*, 2020, **59**, 7830–7835.
- 59 E. Falcone, A. G. Ritacca, S. Hager, H. Schueffl, B. Vileño, Y. El Khoury, P. Hellwig, C. R. Kowol, P. Heffeter, E. Sicilia and P. Faller, *J. Am. Chem. Soc.*, 2022, **144**, 14758–14768.
- 60 P. Wu, *ACS Chem. Biol.*, 2022, **17**, 2959–2961.
- 61 V. Hong, S. I. Presolski, C. Ma and M. G. Finn, *Angew. Chem. Int. Ed.*, 2009, **48**, 9879–9883.
- 62 G. Qiu, P. Nava, A. Martinez and C. Colomban, *Chem. Commun.*, 2021, **57**, 2281–2284.
- 63 T. G. Breve, M. Filius, C. Araman, M. P. van der Helm, P. Hagedoorn, C. Joo, S. I. van Kasteren and R. Eelkema, *Angew. Chem. Int. Ed.*, 2020, **59**, 9340–9344.
- 64 Z. Zhu, H. Chen, S. Li, X. Yang, E. Bittner and C. Cai, *Catal. Sci. Technol.*, 2017, **7**, 2474–2485.
- 65 T. V. Tran, G. Couture and L. H. Do, *Dalton Trans.*, 2019, **48**, 9751–9758.



- 66 G. Qiu, P. Nava, C. Colomban and A. Martinez, *Front. Chem.*, 2020, **8**, 599893.
- 67 M. J. Hardie, *Chem. Soc. Rev.*, 2010, **39**, 516-527.
- 68 J. Canceill, A. Collet, J. Gabard, G. Gottarelli, G. P. Spada, *J. Am. Chem. Soc.* 1985, **107**, 1299-1308.
- 69 C. Colomban, B. Châtelet and A. Martinez, *Synthesis*, 2019, **51**, 2081-2099.
- 70 D. Zhang, B. Bousquet, J.-C. Mulatier, D. Pitrat, M. Jean, N. Vanthuyne, L. Guy, J.-P. Dutasta and A. Martinez, *J. Org. Chem.*, 2017, **82**, 6082-6088.
- 71 G. Qiu, C. Colomban, N. Vanthuyne, M. Giorgi and A. Martinez, *Chem. Commun.*, 2019, **55**, 14158-14161.
- 72 G. Qiu, D. E. Khatmi, A. Martinez and P. Nava, *RSC Adv.*, 2021, **11**, 13763-13768.
- 73 G. Mukherjee, J. K. Satpathy, U. K. Bagha, M. Q. E. Mubarak, C. V. Sastri and S. P. de Visser, *ACS Catal.*, 2021, **11**, 9761-9797.
- 74 Z. Wojdyla and T. Borowski, *Chem. Eur. J.*, 2022, **28**, e202104106.
- 75 M. W. Drover, *Chem. Soc. Rev.*, 2022, **51**, 1861-1880.
- 76 M. Bhadra, J. Yoon, C. Lee, R. E. Cowley, S. Kim, M. A. Siegler, E. I. Solomon and K. D. Karlin, *J. Am. Chem. Soc.*, 2018, **140**, 9042-9045.
- 77 D. E. Diaz, D. A. Quist, A. E. Herzog, A. W. Schaefer, I. Kipouros, M. Bhadra, E. I. Solomon and K. D. Karlin, *Angew. Chem. Int. Ed.*, 2019, **58**, 17572-17576.
- 78 M. A. Ehdin, A. W. Schaefer, S. M. Adam, D. A. Quist, D. E. Diaz, J. A. Tang, E. I. Solomon and K. D. Karlin, *Chem. Sci.*, 2019, **10**, 2893-2905.
- 79 L. Vicens, G. Olivo and M. Costas, *Angew. Chem. Int. Ed.*, 2022, **61**, e2021149.
- 80 G. Olivo, G. Capocasa, B. Ticconi, O. Lanzalunga, S. Di Stefano and M. Costas, *Angew. Chem. Int. Ed.*, 2020, **59**, 12703-12708.
- 81 G. Olivo, G. Farinelli, A. Barbieri, O. Lanzalunga, S. Di Stefano and M. Costas, *Angew. Chem. Int. Ed.*, 2017, **56**, 16347-16351.
- 82 G. De Leener, D. Over, C. Smet, D. Cornut, A. G. Porras-Gutierrez, I. López, B. Douziech, N. Le Poul, F. Topić, K. Rissanen, Y. Le Mest, I. Jabin and O. Reinaud, *Inorg. Chem.* 2017, **56**, 10971-10983.
- 83 P. Aoun, N. Nyssen, S. Richard, F. Zhurkin, I. Jabin, B. Colasson and O. Reinaud, *Chem. Eur. J.* 2022, e202202934.
- 84 Y. Liu, W. Zhao, C.-H. Chen and A. H. Flood, *Science*, 2019, **365**, 159-161.
- 85 G. Qiu, D. Diao, L. Chaussy, S. Michaud-Chevallier, A. J. Simaan, P. Nava, A. Martinez and C. Colomban, *Dalton Trans.*, 2022, **51**, 10702-10706.

